New Journal of Physics
The open access journal at the forefront of physics

Deutsche Physikalische Gesellschaft DPG IOP Institute of Physics

PAPER • OPEN ACCESS

Impact of temperature-dependent local and global spin order in $R\mathrm{MnO}_3$ compounds for spin–phonon coupling and electromagnon activity

To cite this article: S Elsässer *et al* 2017 *New J. Phys.* **19** 013005

IOP Publishing New J. Phys. 19 (2017) 013005 doi:10.1088/1367-2630/aa55ed

New Journal of Physics
The open access journal at the forefront of physics

Deutsche Physikalische Gesellschaft DPG
IOP Institute of Physics

Published in partnership with: Deutsche Physikalische Gesellschaft and the Institute of Physics

OPEN ACCESS

RECEIVED
7 November 2016

REVISED
22 December 2016

ACCEPTED FOR PUBLICATION
28 December 2016

PUBLISHED
9 January 2017

PAPER

Impact of temperature-dependent local and global spin order in $R\mathrm{MnO_3}$ compounds for spin–phonon coupling and electromagnon activity

S Elsässer[1], M Schiebl[2], A A Mukhin[3], A M Balbashov[4], A Pimenov[2] and J Geurts[1]

[1] Physikalisches Institut (EP3), Universität Würzburg, D-97074 Würzburg, Germany
[2] Institute of Solid State Physics, Vienna University of Technology, A-1040 Vienna, Austria
[3] Prokhorov General Physics Institute, Russian Academy of Sciences, 119991 Moscow, Russia
[4] Moscow Power Engineering Institute (Technical University), ul. Krasnokazarmennaya 14, Moscow 111250, Russia

E-mail: sebastian.elsaesser@physik.uni-wuerzburg.de

Keywords: $R\mathrm{MnO_3}$, multiferroics, electromagnon, Raman spectroscopy, spin–phonon coupling

Abstract

The orthorhombic rare-earth manganite compounds $R\mathrm{MnO_3}$ show a global magnetic order for $T < T_N$, and several representatives are multiferroic with a cycloidal spin ground state order for $T < T_{\mathrm{cycl}} < T_N \approx 40$ K. We deduce from the temperature dependence of spin–phonon coupling in Raman spectroscopy for a series of $R\mathrm{MnO_3}$ compounds that their spin order locally persists up to about twice T_N. Along the same line, our observation of the persistence of the electromagnon in $\mathrm{GdMnO_3}$ up to $T \approx 100$ K is attributed to a local cycloidal spin order for $T > T_{\mathrm{cycl}}$, in contrast to the hitherto assumed incommensurate sinusoidal phase in the intermediate temperature range. The development of the magnetization pattern can be described in terms of an order–disorder transition at T_{cycl} within a pseudospin model of localized spin cycloids with opposite chirality.

1. Introduction

Since the discovery of the giant magnetoelectric effect [1–4], the study of multiferroics, where an electric field E can affect the magnetic properties and vice versa, has gained strong interest [5–13]. While a large number of compounds was shown to exhibit multiferroic behavior, the underlying mechanisms are often still not fully understood. Considering the extensively studied $R\mathrm{MnO_3}$ family of orthorhombically distorted perovskites, the cycloid-type order of the Mn spin ground state is seen as the origin of ferroelectric polarization of the multiferroic members (R = Gd, Tb, Dy) [14–16]. As a prerequisite for a cycloidally ordered magnetic state, frustration needs to be introduced to the spin system to deviate from the conventional parallel or antiparallel ordering of spins. This can be achieved by geometrical frustration as, for example, for antiferromagnetically coupled spins on a triangular or Kagomé lattice, or by competing ferro-(FM) and antiferromagnetic (AFM) exchange interactions [9, 10, 17]. The latter is the case for the orthorhombically distorted $R\mathrm{MnO_3}$ compounds, where the nearest-neighbor Mn–O–Mn exchange within the $\mathrm{MnO_2}$ plane is FM and the next-nearest neighbor interaction along the perpendicular direction is AFM in nature [18]. By choosing R-ions with appropriate ionic radius, the orthorhombic distortion angle can be tuned. With decreasing R-ion radius and therefore increasing orthorhombic distortion angle, the FM in-plane interactions are weakened, while the AFM plane-to-plane interactions are enhanced. For the material series from $\mathrm{LaMnO_3}$ to $\mathrm{EuMnO_3}$, this results in canted A-type antiferromagnetism with T_N-values decreasing from ≈150 K for $\mathrm{LaMnO_3}$ to ≈50 K for $\mathrm{EuMnO_3}$ [18, 19]. The angular range in which the competing FM and AFM contributions are comparable, resulting in a cycloidal spin structure, occurs between $\mathrm{EuMnO_3}$ and $\mathrm{HoMnO_3}$ and comprises the compounds $\mathrm{GdMnO_3}$, $\mathrm{TbMnO_3}$ and $\mathrm{DyMnO_3}$. Besides by these stoichiometric $R\mathrm{MnO_3}$ compounds, this angular range is also achievable by solid solutions of various combinations of R-site ions, which, moreover, allow a fine-tuning of the systems properties, e.g. by $\mathrm{Eu_{1-x}Y_xMnO_3}$ or $\mathrm{Eu_{1-x}Ho_xMnO_3}$ [19, 20]. Within the framework of the inverse

Dzyaloshinskii–Moriya (IDM) model, the non-collinear arrangement of spins induces an electric dipole moment [21]

$$\mathbf{p_{ij}} \propto \mathbf{e_{ij}} \times (\mathbf{S_i} \times \mathbf{S_j}), \tag{1}$$

where $\mathbf{e_{ij}}$ denotes the unit vector which connects the spins $\mathbf{S_i}$ and $\mathbf{S_j}$. This was confirmed by the simultaneous flop of electric polarization, when the cycloid helicity is reversed by application of a magnetic field [22, 23]. Another consequence of the magnetoelectric coupling in a cycloidal structure is the existence of an electric-dipole-active magnon excitation, termed the electromagnon [24–28]. Additionally, especially in $GdMnO_3$, the experimentally observed selection rules for the electromagnon deviate from the expected behavior: when the rotational plane of the spin cycloid is flipped, the selection rule for excitation should flip accordingly. In contrast, it was found that the largest part of the dipole activity was bound to the crystal lattice and not to the cycloidal plane [29], which implies contributions of magnetostrictive nature, according to [15]

$$\mathbf{p_{ij}} \propto (\mathbf{S_i} \cdot \mathbf{S_j}). \tag{2}$$

Thus, for electromagnons generally both IDM and magnetostriction mechanisms may be of relevance. Besides, the magnetic ordering of Mn^{3+} spins may also influence the phonon mode dynamics. This effect is denoted as spin–phonon coupling (SPC). Its experimental analysis essentially occurs by Raman spectroscopy [20, 30–33], where it mostly results in a mode-specific frequency softening with decreasing temperature. This frequency shift is usually assumed to be proportional to the spin-correlations $\Delta\omega_{SPC} \propto \langle \mathbf{S}_i \cdot \mathbf{S}_j \rangle$. Thus, the strongest SPC is expected in systems with full global spin order, but it might also occur to a lesser degree already for local spin order.

It has been argued that the magnetic structure of the various $R\mathrm{MnO_3}$ compounds changes with increasing temperature from the cycloidal ground state below $T_{cycl} \approx 28$ K to an intermediate sinusoidal collinear phase ($T_{cycl} < T < T_N$) before arriving at the paramagnetic state[5] ($T > T_N \approx 40$ K) [7]. A (static) sinusoidal order, however, does not agree with the fact, that Mn^{3+} should exhibit a Heisenberg spin with constant magnitude of $S = 2$. A more satisfying approach is to view the sinusoidal order as a time-averaged mixture of cycloidal phases, as suggested by model calculations [19] and by analysis of dielectric relaxation [34]. This raises the question about the underlying nature of the intermediate magnetic order above T_{cycl} and how the transition from the low-temperature cycloidal phase to the paramagnetic phase takes place.

We have investigated the temperature-dependent behavior of phonons and electromagnons on multiferroic $R\mathrm{MnO_3}$ compounds by Raman and THz spectroscopy, respectively. Our results suggest that the cycloidal phase extends on a short-range scale towards much higher temperatures than T_{cycl}, and local cycloidal order persists even distinctly above $T_N \approx 40$ K. This is evidenced by the observation of the persistence of both the electromagnon and the SPC up to temperatures around 100 K. Furthermore, a characteristic activation energy of $E_A \approx 100$ K for switching between cycloid chirality in the pseudospin model was found for $DyMnO_3$ by dielectric spectroscopy [34]. Additionally, it was reported by De *et al* [35] that the polarization of a poled sample is preserved up to about 90 K, which further indicates the presence of cycloids up to this temperature. Therefore we propose that the underlying order of the sinusoidal and even of the paramagnetic phase may be explained as a dynamical equilibrium of fluctuating cycloids with opposite chirality. Along the same line, we observe also for non-multiferroic $R\mathrm{MnO_3}$ compounds a persistence of SPC up to about 100 K, which implies the occurrence of local spin order far above T_N also in this case.

2. Experimental

The orthorhombically distorted $R\mathrm{MnO_3}$ samples were grown by a floating zone method. Within the *Pnma* coordinate axes orientation (International tables orientation) the alternating MnO_2- and *R*O-planes are denoted as (*a*, *c*)-planes, while the axis perpendicular to these planes is called the *b*-axis. The polarized Raman spectra for the SPC studies were recorded from (*a*, *c*) surfaces (*b*-cut samples) and from (*b*, *c*) surfaces (*a*-cut samples), using a Horiba LabRAM HR 800 spectrometer equipped with a notch filter, a Peltier-cooled CCD camera as detector, and a 632.8 nm He–Ne laser for excitation. Laser focusing as well as signal collection was performed using a microscope with a 50× ULWD objective. To obtain the temperature-dependent spectra (5 K $\leqslant T \leqslant$ 295 K), the samples were mounted inside a LHe-flow cryostat. The terahertz and far-infrared spectra of the electromagnons were obtained on thin plane-parallel samples in transmittance geometry with a Mach–Zehnder type interferometer, with backward-wave oscillators providing the monochromatic, linearly polarized radiation sources. For detection, either a Golay cell or a liquid-He-cooled bolometer was used. Further details of this technique are provided in [36].

[5] T_{cycl} and T_N should not be confused with the Jahn–Teller temperature which exceeds 1000 K for the considered $R\mathrm{MnO_3}$ compounds [47].

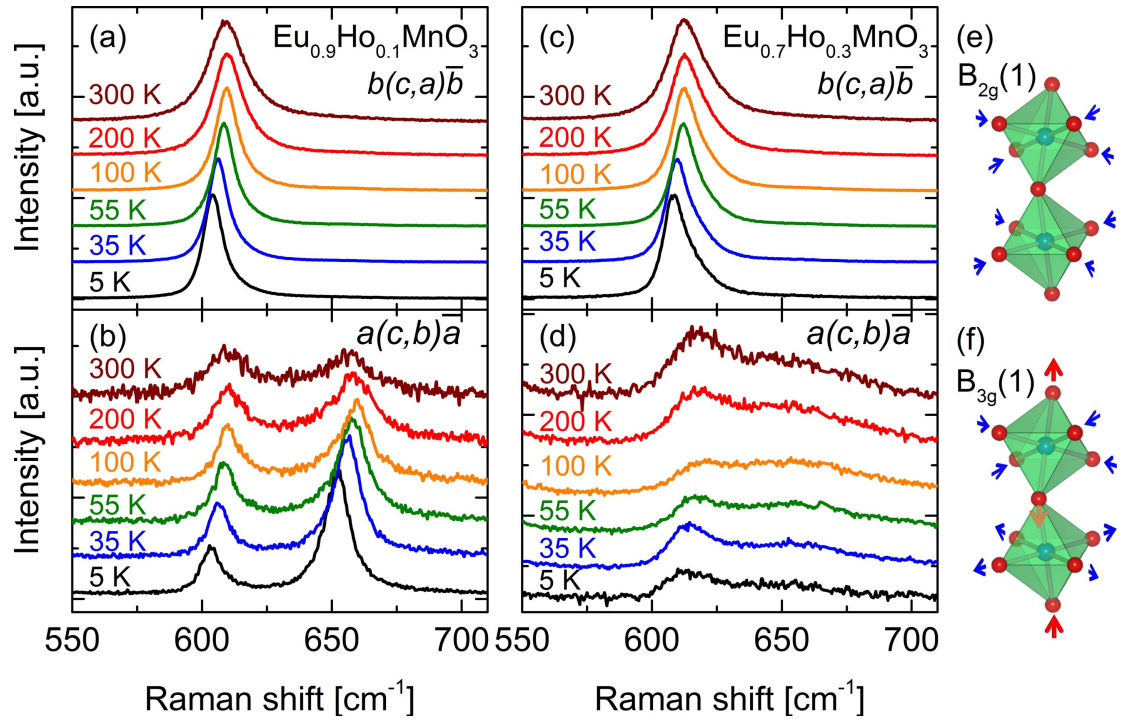

Figure 1. Temperature-dependent polarized Raman spectra for ((a) and (b)) $Eu_{0.9}$ $Ho_{0.1}MnO_3$ and ((c) and (d)) $Eu_{0.7}$ $Ho_{0.3}MnO_3$. The spectral range comprises the octrahedron breathing modes $B_{2g}(1)$ ($\approx$610 cm^{-1}) and $B_{3g}(1)$ ($\approx$660 cm^{-1}). ((e) and (f)) octahedron elongation patterns for $B_{2g}(1)$ (e) and $B_{3g}(1)$ (f).

3. Results and discussion

3.1. Spin–phonon coupling

We have analyzed the temperature dependence of the SPC strength for various multiferroic and non-multiferroic $RMnO_3$ compounds: the stoichiometric $EuMnO_3$, $GdMnO_3$, and $TbMnO_3$, as well as the doped (Eu, Y)MnO_3 and (Eu, Ho)MnO_3 with various compositions. Here, we present in detail the results on $Eu_{1-x}Ho_xMnO_3$, which is multiferroic for $x > 0.2$ [37]. Details of the SPC results of the other compounds can be found elsewhere [31, 38].

Figure 1 shows temperature-dependent polarized Raman spectra for $Eu_{0.9}Ho_{0.1}MnO_3$ and $Eu_{0.7}$ $Ho_{0.3}MnO_3$ as an example for SPC-induced frequency renormalization of the octahedron breathing mode $B_{2g}(1)$ ($\approx$610 cm^{-1}). The former sample is in close vicinity to the multiferroic phase, the latter within the multiferroic region. Its orthorhombic distortion angle is located between those of the stoichiometric multiferroic compounds $GdMnO_3$ and $TbMnO_3$. As shown in figure 1(e), the $B_{2g}(1)$ mode consists of breathing movements of the MnO_2 oxygen ions which are in-phase along the *b*-direction. Thus, this mode can be used to probe the in-plane FM magnetic correlations within the *ac*-plane. In contrast, within the $B_{3g}(1)$ mode the MnO_2 breathing movements are out-of-phase and, additionally, the apical oxygen ions move along the *b*-axis (figure 1(f)). As the interaction along the *b*-axis is AFM, this mode in conjunction with the $B_{2g}(1)$ mode allows to disentangle the FM from the AFM interaction strength as described in detail elsewhere [39]. Here, we will focus solely on the temperature-dependent frequency shift of the $B_{2g}(1)$ mode which is induced by the SPC, as the cycloidal order is oriented within the ac planes. The phonon peak positions in figure 1 are clearly temperature dependent. Upon cooling down from 300 K, the peak frequency is first increased due to the common reduced anharmonic decay, followed upon further cooling by a decrease, which can be attributed to SPC. This behavior is plotted quantitatively in figure 2, which shows the *T*-dependence of the $B_{2g}(1)$ eigenfrequency values for $x = 0.1$ and $x = 0.3$ in the insets of figures 2(b) and (c), respectively. For comparison, the corresponding data for stoichiometric $EuMnO_3$, i.e., $x = 0$, are plotted in the inset of figure 2(a). For the quantitative separation of the contribution of magnetic correlations to the temperature dependence from the intrinsic temperature-dependent phonon behavior due to the anharmonic decay of an optical phonon into two acoustic ones, we apply the anharmonic-decay-based formula [40, 41]:

$$\omega(T) = \omega_0 - C\left[1 + \frac{2}{e^{\frac{\hbar\omega^*}{2k_BT}} - 1}\right] \quad (3)$$

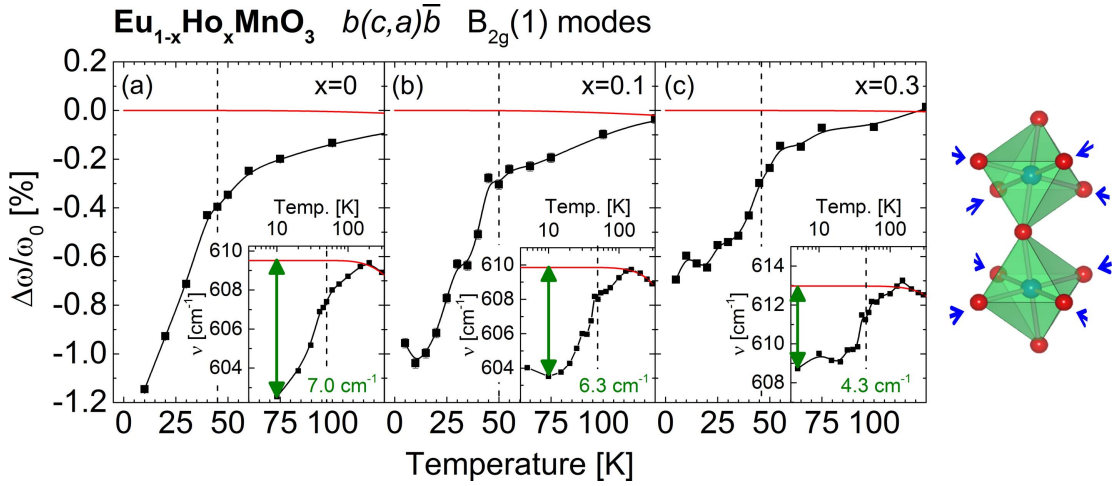

Figure 2. Renormalization of $B_{2g}(1)$ phonon frequencies of $Eu_{1-x}Ho_xMnO_3$ for (a) $x = 0$, (b) $x = 0.1$, and (c) $x = 0.3$, relative to the extrapolated frequency $\omega(T \to 0)$ obtained by equation (3). The deviation from the fits (red curves) according to equation (3) is caused by spin–phonon coupling. The insets show the $B_{2g}(1)$ frequencies with their fits up to room temperature and the maximum absolute SPC-induced shifts, indicated by green arrows. The dashed vertical lines indicate T_N.

also referred to as Klemens model. Here, $\omega_0 = (\omega^* - C)$ is the wavenumber of the phonon for $T \to 0$ and C is a free parameter that describes the strength of the anharmonic decay. This formula is expected to fit to the experimental data in absence of the magnetic order. The deviation from this curve will be ascribed to SPC, i.e., a phonon frequency renormalization, caused by magnetic correlations. The fits according to the Klemens formula are shown in figure 2 as red curves. They describe very well the experimentally observed cooling-induced increasing eigenfrequencies data in the upper temperature range (see insets). However, for lower temperatures the model predicts a constant frequency, while the experimental data show upon further cooling a clear redshift.

The frequency renormalization strengths, i.e., relative frequency shifts of the $B_{2g}(1)$ modes with respect to the $(T = 0)$ frequency from the Klemens-fits are shown in the main panels of figure 2. The redshift of the eigenfrequencies amounts up to ≈1%. This SPC-induced frequency shift $\Delta\omega_{SPC}(T) = \omega_0 - \omega(T)$ is proportional to the spin correlations

$$\Delta\omega_{SPC} \propto \langle \mathbf{S}_i \cdot \mathbf{S}_j \rangle. \quad (4)$$

Obviously, according to equation (4), SPC is not confined to a global cycloidal magnetic order. Therefore, it also occurs for non-multiferroics, such as $EuMnO_3$ (figure 2(a)) and $Eu_{0.9}$ $Ho_{0.1}MnO_3$ (figure 2(b)), which show A-type antiferromagnetic order [37]. It was shown before, that SPC is directly related to the distortion angle between adjacent octahedra and therefore reflects magnetic correlations at a local level [38].

A key result of our study is the observation of SPC as a clear deviation from equation (3) not only for the ordered phase below T_N, but also far above the long-range-order temperature T_N, up to about 100 K, indicating local spin correlations even at this elevated temperature. This is in contrast to an abrupt ordering of spins at T_N or T_{cycl}. There is no abrupt anomaly in the phonon behavior at both temperatures, which would correspond to a phase transition. We have obtained similar results for the multiferroics $GdMnO_3$ and $TbMnO_3$, as well as for doped (Eu,Y)MnO_3 with various compositions [31, 38]. The corresponding values of T_N and the temperature ranges for the onset of SPC are listed in table 1. For all investigated compounds the temperature range of the SPC onset exceeds T_N by far, for most of them by a factor of two or even more. Besides, we want to point out that the Raman data of several other research groups show SPC at $T \gg T_N$ generally for $RMnO_3$ compounds, e.g. for $DyMnO_3$ with $T_N = 40$ K and $T_{SPC} \approx 120$ K [32] and several others [32, 42, 43], but in none of these reports this observation is discussed in terms of Mn-spin order in this temperature range. In our opinion all existing results on the temperature dependence of SPC in $RMnO_3$ can be explained consistently by assuming a that this SPC is due to local, short-range order of the Mn spins, persisting far above the Néel temperature.

3.2. Electromagnon activity

The interpretation given above is supported by our THz data for electromagnons in $GdMnO_3$ as shown in figure 3. Interestingly, $GdMnO_3$ is a material with no clearly established cycloidal phase [24]. However, well defined electromagnons at Terahertz frequencies strongly suggest the existence of at least a disordered cycloid. In contrast to the similar compound $DyMnO_3$, the disorder does not allow the observation of static electric

Table 1. Magnetic order temperatures T_N and approximate temperatures T_{SPC} for the onset of spin–phonon coupling obtained by Raman spectroscopy [31, 38]. Spin-correlations are present even at $T \gg T_N$.

	T_N (K)	T_{SPC} (K)
$EuMnO_3$	50	100–130
$Eu_{0.9}Y_{0.1}MnO_3$	48	100–120
$Eu_{0.8}Y_{0.2}MnO_3$	47	100
$Eu_{0.7}Y_{0.3}MnO_3$	46	100–110
$Eu_{0.6}Y_{0.4}MnO_3$	46	50–60
$Eu_{0.5}Y_{0.5}MnO_3$	45	50–60
$GdMnO_3$	45	80
$TbMnO_3$	42	50–60

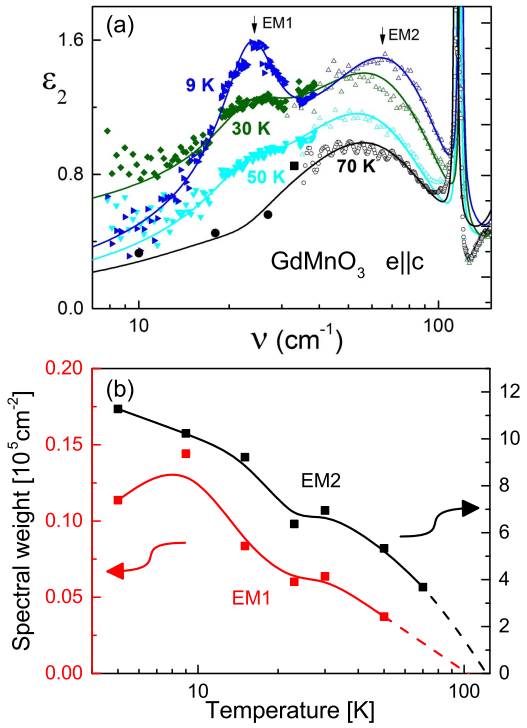

Figure 3. (a): Terahertz and infrared permittivity of $GdMnO_3$ below and above the magnetically ordered state at $T_N \approx 40$ K. Two electromagnon modes are marked as EM1 and EM2. The sharp mode around 120 cm^{-1} is an infrared phonon (adapted from [44]). (b): spectral weight of two low-frequency electromagnons in $GdMnO_3$ as obtained from the spectra in panel (a). Red symbols: mode at 25 cm^{-1} (THz data), black symbols: mode at 80 cm^{-1} (infrared results). Lines are guides to the eye and they demonstrate the characteristic energy scale of 100 K.

polarization. In $GdMnO_3$ the electromagnons are observed up to 70 K as shown in figure 3(a). The intensity of the electromagnon modes has been estimated by fitting the data using a sum of Lorentzian modes and is given as the spectral weight of the modes, which is defined as

$$SW = \int_0^\infty \mathrm{Re}(\sigma(\omega))\,\mathrm{d}\omega. \tag{5}$$

In case of a Lorentzian the spectral weight is equal to

$$SW = \frac{\pi}{2}\varepsilon_0 \Delta\varepsilon \cdot \omega_0^2, \tag{6}$$

where ε_0 is the permittivity of vacuum, $\Delta\varepsilon$ and ω_0 are dielectric contribution and eigenfrequency of the Lorentzian, respectively. As demonstrated in figure 3(b), the extrapolation of the electromagnon spectral weight suggests nonzero spectral weight up to ≈100 K. This continuous decrease of the electromagnon intensity indicates the existence of spin cycloids until much higher temperatures than $T_N \approx 40$ K.

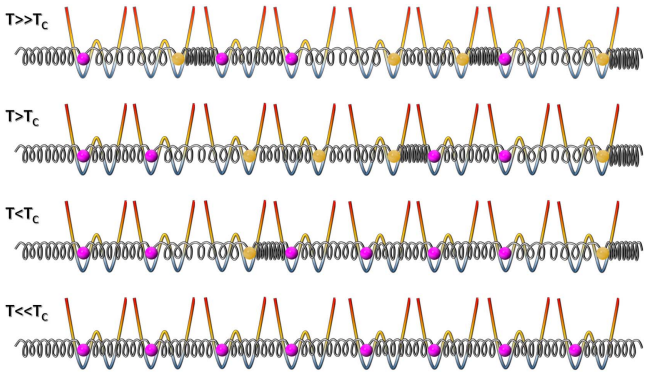

Figure 4. Sequence showing the ordering of atoms in the order–disorder limit in a double-well potential model with a critical temperature T_C. In our system, T_C represents the global cycloid ordering temperature T_{cycl}. At high temperatures ($T \geqslant T_C$) the positions of neighboring ions are not correlated in any significant way (magenta and yellow balls indicate ions in the left or in the right state of the double-well potential, respectively). Near the transition temperature a degree of short-range order is established. Below the transition temperature one side of the double-well potential is favored and a long-range order appears. Well below the transition temperature each ion occupies the same side of the double-well potential.

3.3. Order–disorder limit: the pseudo-spin model

A useful idea explaining the continuation of the magnetoelectric characteristics of multiferroic manganites into the paramagnetic phase is given by the pseudo-spin model [34]. In short, this model exactly reproduces the main results discussed above: (i) both the sinusoidal magnetic structure and the paramagnetic state below $T \approx 100$ K should be described as a mixture of the magnetic cycloids with opposite chiralities. (ii) The characteristic energy scale of the problem is not given by $T_N \approx 40$ K but is rather $E_A \simeq 100$ K. The pseudo-spin model [34] has been developed and applied for dielectric relaxation in $DyMnO_3$ and it is based on the relation between the spin-induced electric polarization and the chirality of the magnetic cycloid [22, 28]. Within this model, the polarization in the ferroelectric phase is proportional to the difference of opposite chiralities of Mn^{3+} magnetic cycloids. Hence, the electric polarization can be considered as the primary order parameter of the system. In addition, an order–disorder type phase transition between paraelectric and ferroelectric states is suggested. The main idea of the pseudo-spin model is illustrated in figure 4. Here, (i) the electric dipole moments are associated with the displacement of the O^{2-} ions due to inverse DM interaction [22, 28], (ii) the direction of the electric dipoles depends on the chirality of the magnetic order, (iii) the two possible directions of the electric dipoles are separated by an energy barrier E_A and are coupled. In the order–disorder limit ($E_A/k_B T_{cycl} > 1$ [45, 46]), the system can be described by the pseudospin formalism, the model Hamiltonian is essentially of Ising-type and may be written as:

$$H \propto -\sum_{R,R'} \Delta x^2 J_{R,R'} \sigma_R \sigma_{R'} \tag{7}$$

where Δx is the displacement of the O^{2-} ion, $J_{R,R'}$ is the coupling constant between O^{2-} ions at position R and R', and σ_R is the pseudospin at position R with $\sigma_R = x_R/\Delta x$, which can take the values $+1$ and -1 (figure 4), E_A is the activation energy determining the characteristic temperature scale (the height of the energy barrier).

From the viewpoint of the order parameter dynamics the jumps between the minima of the potential wells in figure 4 are of main interest since this motion of ions implicates the flipping of pseudo-spins.

An analysis of the relaxation characteristics of $DyMnO_3$ near the magnetically induced ferroelectric phase transition which was performed according to the pseudo-spin model, confirmed an order-disorder type transition with an experimentally determined activation energy of $E_A \approx 100$ K [34]. Thus, for temperatures $T < E_A$, the ions reside in one or the other side of the double-well potential and a local cycloidal spin order is present due to IDM. On the other hand, for temperatures $T \geqslant E_A$, the local potential does not force ions to stay on one side of the double-well potential. Instead, the ions vibrate around the averaged position, and the shape of the double-well potential has only a small effect to modify the phonon frequencies. Consequently, due to IDM interaction, the neighboring Mn^{3+} spins must align collinearly ($\mathbf{S}_i \times \mathbf{S}_{i+1} = 0$) and no local cycloidal spin order is present.

4. Summary

The analysis of the temperature dependence of the SPC strength in a series of various $RMnO_3$ compounds shows no abrupt disappearance at T_N, but in contrast the persistence of local order of the Mn-spins up to $T \approx 100$ K. This is far above T_N and even further above the phase transition at T_{cycl} for the multiferroic representatives. This

observation is underscored by the temperature dependence of the spectral weight of electromagnon excitations in $GdMnO_3$, which is explained by describing the evolution of the magnetic structure of a multiferroic compound with increasing temperature as a pseudo-spin system of two possible types of cycloids with opposite chirality, which locally persist up to around 100 K. Because of this local character, the temperature scale of 100 K is not to be understood as a phase transition, but rather as a gradual onset of local order. Thus, the phonons and the electromagnons serve as valuable quasi-local probes, revealing the development of the magnetic correlation between neighboring spins even in the absence of global magnetic order.

Acknowledgments

This work was funded by Deutsche Forschungsgemeinschaft (DFG) Grant No. GE1855/13-1 and the Austrian Science Fund (Grants No. I815-N16 and No. W-1243).

References

[1] Tokura Y, Urushibara A, Moritomo Y, Arima T, Asamitsu A, Kido G and Furukawa N 1994 *J. Phys. Soc. Japan* **63** 3931–5
[2] von Helmolt R, Wecker J, Holzapfel B, Schultz L and Samwer K 1993 *Phys. Rev. Lett.* **71** 2331–3
[3] Ishihara S, Inoue J and Maekawa S 1997 *Phys. Rev.* B **55** 8280–6
[4] Kimura T, Goto T, Shintani H, Ishizaka K, Arima T and Tokura Y 2003 *Nature* **426** 55–8
[5] Fiebig M 2005 *J. Phys. D: Appl. Phys.* **38** R123–52
[6] Eerenstein W, Mathur N D and Scott J F 2006 *Nature* **442** 759–65
[7] Kenzelmann M, Harris A B, Jonas S, Broholm C, Schefer J, Kim S B, Zhang C L, Cheong S W, Vajk O P and Lynn J W 2005 *Phys. Rev. Lett.* **95** 087206
[8] Rao C N R, Sundaresan A and Saha R 2012 *J. Phys. Chem. Lett.* **3** 2237–46
[9] van den Brink J and Khomskii D I 2008 *J. Phys.: Condens. Matter* **20** 434217
[10] Tokura Y and Seki S 2010 *Adv. Mater.* **22** 1554–65
[11] Tokura Y, Seki S and Nagaosa N 2014 *Rep. Prog. Phys.* **77** 076501
[12] Dong S and Liu J M 2012 *Mod. Phys. Lett.* B **26** 1230004
[13] Kováčik R, Murthy S S, Quiroga C E, Ederer C and Franchini C 2016 *Phys. Rev.* B **93** 075139
[14] Kimura T 2007 *Annu. Rev. Mater. Res.* **37** 387–413
[15] Mostovoy M 2006 *Phys. Rev. Lett.* **96** 067601
[16] Mochizuki M, Furukawa N and Nagaosa N 2011 *Phys. Rev.* B **84** 144409
[17] Arima T 2007 *J. Phys. Soc. Japan* **76** 073702
[18] Kimura T, Ishihara S, Shintani H, Arima T, Takahashi K T, Ishizaka K and Tokura Y 2003 *Phys. Rev.* B **68** 060403
[19] Mochizuki M and Furukawa N 2009 *Phys. Rev.* B **80** 134416
[20] Hemberger J, Schrettle F, Pimenov A, Lunkenheimer P, Ivanov V Y, Mukhin A A, Balbashov A M and Loidl A 2007 *Phys. Rev.* B **75** 035118
[21] Sergienko I A and Dagotto E 2006 *Phys. Rev.* B **73** 094434
[22] Zhao T *et al* 2006 *Nat. Mater.* **5** 823–9
[23] Kagawa F, Mochizuki M, Onose Y, Murakawa H, Kaneko Y, Furukawa N and Tokura Y 2009 *Phys. Rev. Lett.* **102** 057604
[24] Pimenov A, Mukhin A A, Ivanov V Y, Travkin V D, Balbashov A M and Loidl A 2006 *Nat. Phys.* **2** 97–100
[25] Sushkov A B, Aguilar R V, Park S, Cheong S W and Drew H D 2007 *Phys. Rev. Lett.* **98** 027202
[26] Aguilar R V, Mostovoy M, Sushkov A B, Zhang C L, Choi Y J, Cheong S W and Drew H D 2009 *Phys. Rev. Lett.* **102** 047203
[27] Mochizuki M, Furukawa N and Nagaosa N 2010 *Phys. Rev. Lett.* **104** 177206
[28] Cheong S W and Mostovoy M 2007 *Nat. Mater.* **6** 13–20
[29] Shuvaev A M, Travkin V D, Ivanov V Y, Mukhin A A and Pimenov A 2010 *Phys. Rev. Lett.* **104** 097202
[30] Granado E, García A, Sanjurjo J A, Rettori C, Torriani I, Prado F, Sánchez R D, Caneiro A and Oseroff S B 1999 *Phys. Rev.* B **60** 11879–82
[31] Issing S, Pimenov A, Ivanov V Y, Mukhin A A and Geurts J 2010 *Phys. Rev.* B **81** 024304
[32] Laverdière J, Jandl S, Mukhin A A, Ivanov V Y, Ivanov V G and Iliev M N 2006 *Phys. Rev.* B **73** 214301
[33] Sushkov A B, Tchernyshyov O, II W R, Cheong S W and Drew H D 2005 *Phys. Rev. Lett.* **94** 137202
[34] Schiebl M, Shuvaev A, Pimenov A, Johnstone G E, Dziom V, Mukhin A A, Ivanov V Y and Pimenov A 2015 *Phys. Rev.* B **91** 224205
[35] De C and Sundaresan A 2015 *Appl. Phys. Lett.* **107** 052902
[36] Shuvaev A M, Mayr F, Loidl A, Mukhin A A and Pimenov A 2011 *Eur. Phys. J.* B **80** 351–4
[37] Ivanov V Y, Mukhin A A, Glushkov V V and Balbashov A M 2013 *JETP Lett.* **97** 28–33
[38] Issing S, Pimenov A, Ivanov Y V, Mukhin A A and Geurts J 2010 *Eur. Phys. J.* B **78** 367–72
[39] Elsässer S, Geurts J, Mukhin A A and Balbashov A M 2016 *Phys. Rev.* B **93** 054301
[40] Balkanski M, Wallis R F and Haro E 1983 *Phys. Rev.* B **28** 1928–34
[41] Klemens P G 1966 *Phys. Rev.* **148** 845
[42] Rovillain P, Liu J, Cazayous M, Gallais Y, Measson M A, Sakata H and Sacuto A 2012 *Phys. Rev.* B **86** 014437
[43] Vilarinho R, Queiros E C, Almeida A, Tavares P B, Guennou M, Kreisel J and Agostinho Moreira J 2015 *J. Solid State Chem.* **228** 76–81
[44] Pimenov A, Shuvaev A M, Mukhin A A and Loidl A 2008 *J. Phys.: Condens. Matter* **20** 434209
[45] Lawes G, Ramirez A P, Varma C M and Subramanian M A 2003 *Phys. Rev. Lett.* **91** 257208
[46] Muralidharan R, Jang T H, Yang C H, Jeong Y H and Koo T Y 2007 *Appl. Phys. Lett.* **90** 012506
[47] Zhou J S and Goodenough J B 2006 *Phys. Rev. Lett.* **96** 247202